International Journal of Mass Spectrometry 285 (2009) 12–18

Contents lists available at ScienceDirect

International Journal of Mass Spectrometry

journal homepage: www.elsevier.com/locate/ijms

Charged particle formation by the ionization of air containing sulfur dioxide

Kenkichi Nagato*

Department of Mechanical Engineering, Kochi National College of Technology, Monobe 200-1, Nankoku 783-8508, Japan

ARTICLE INFO

Article history:
Received 12 January 2009
Received in revised form 25 February 2009
Accepted 25 February 2009
Available online 13 March 2009

Keywords:
Ion-induced nucleation
Corona discharge
Non-thermal plasma
Ion-molecule reaction
Charger

ABSTRACT

Experimental investigation of charged particle formation by the ionization of air containing sulfur dioxide (SO_2) was performed using a nano-DMA (differential mobility analyzer) and an atmospheric pressure ionization mass spectrometer. A radioactive ion source of ^{241}Am and a negative dc corona discharge were used to ionize SO_2/H_2O/air mixtures. The results showed that the number of charged particles that formed had increased as H_2O concentration increased (ca. $20–3 \times 10^3$ ppm) for both ion sources, but also that the number of charged particles produced when using the negative corona discharge was more than two orders of magnitude greater than what was produced using ^{241}Am. During ionization by α-ray irradiation, $SO_4^-(H_2O)_n$ ions predominated coincident with the formation of charged particles. The negative corona discharge produced a more complicated ion mass spectrum, which included ion groups of NO_3^-, SO_x^- ($x = 2–5$) and HSO_x^- ($x = 3–5$). The relative abundance of the ion groups varied depending on H_2O concentration and ion reaction time. The ions with an HSO_4^- core surpassed the ions of other groups as H_2O concentration increased. The formations of NO_3^- ions and cluster ions containing HNO_3 also were enhanced at higher H_2O concentrations. Possible ion-molecule reactions responsible for the observed mass spectra are discussed in detail.

1. Introduction

The ionization of air is known to promote nucleation. This is primarily due to the formation of gaseous ions. Electrostatic force helps to form stable ion clusters and lowers the nucleation barrier. Therefore, the ion-induced nucleation process is thermodynamically more favorable than the homogeneous nucleation process. Another reason is that the ionization of air yields not only ions but other active species as well, such as radicals and excited molecules, which can oxidize some kinds of molecules in air to form condensable compounds.

Ion-induced nucleation has been suggested as a possible mechanism for atmospheric aerosol formation [1]. The earth's atmosphere is continuously ionized by cosmic rays. Near the ground surface, the decay of radioactive gases is another ionizing agent. As a result, gaseous ions are ubiquitous even in the lower atmosphere. Mass spectrometric measurements have revealed the ions of sulfuric acid (HSO_4^-) to be the dominant negative ion species at ground level [2,3], and ion-induced nucleation involving HSO_4^- ions is believed to contribute to some of the observed events of new particle formation [4,5]. Since sulfur dioxide (SO_2) is a precursor of gaseous sulfuric acid (H_2SO_4), experiments on particle formation by the ionization of air containing SO_2 have been conducted to simulate atmospheric ion-induced nucleation in the laboratory.

The study of particle formation from SO_2 using ionizing irradiation is also important in understanding the fundamental process of the desulfurization of flue gases with non-thermal plasmas (NTP) [6–8]. NTP can be generated using various types of electrical discharges or electron beams. High-energy electrons formed in NTP efficiently produce reactive radicals, mainly OH radicals, through dissociation, excitation and ionization of N_2, O_2 and H_2O. OH radicals play a central role in the conversion of SO_2 into H_2SO_4. In addition, reaction with surrounding negative ions tends to chemically ionize H_2SO_4 to form HSO_4^-, which is believed to nucleate effectively into fine particles via ion-induced nucleation.

A number of experimental studies have focused on particle formation by the ionization of air with SO_2 [9–14]. The ion sources employed in those studies include the following: α-, γ- and X-rays; corona discharge; and a spray ion source. Despite these efforts, only limited information is available about the kinetics of the reactions involving SO_2 because most of the past studies focused only on the measurement of particles. To investigate the kinetics of SO_2 reactions that are initiated by ionization, an analysis of neutral compounds or ions originating from SO_2 is needed. In particular, mass spectrometric measurements of negative ions are expected to provide useful information because the products resulting from SO_2 generally tend to be negative ions. Recent research has proven that atmospheric ionization mass spectrometry is a powerful technique

* Tel.: +81 88 864 5641; fax: +81 88 864 5641.
E-mail address: nagato@me.kochi-ct.ac.jp.

1387-3806/$ – see front matter © 2009 Elsevier B.V. All rights reserved.
doi:10.1016/j.ijms.2009.02.025

for the investigation of ion-molecule reactions occurring in air with corona sources operated under atmospheric pressure [15–17].

In this study, we investigated the formation process of charged particles by the ionization of air containing SO_2. To analyze the chemical kinetics involving SO_2 and the early stages of particle formation, we measured negative ion composition and the size distribution of charged particles as a function of H_2O concentration. In our previous study, we developed a measurement system employing an ion mobility spectrometer/mass spectrometer (IMS/MS) and a nano-DMA for ions and charged particles generated by ionization in air [18]. We used this same system for the present study.

The ion sources used in this study were ^{241}Am and negative dc corona discharge, which are widely used in the field of aerosol science as bipolar and unipolar chargers, respectively [19,20]. Knowledge of potential particle formation by aerosol chargers is crucial for precise particle measurement if the carrier gas contains impurities that can be transformed into condensable compounds by the effects of ionization. In this respect, the results of this study can be used to evaluate the particle formation capability of aerosol chargers using ^{241}Am and negative corona discharge.

2. Experimental

Fig. 1 shows the experimental arrangement used in the present study, the details of which have been described previously [18,21]. All measurements were conducted under room temperature. For charged-particle measurement, the SO_2/H_2O/air mixtures were ionized in a small ion source chamber, into which was placed either a disk of ^{241}Am (3.03 MBq) or a corona ionizer. The corona ionizer used in this study consisted of a discharge needle and a ring electrode (12 mm i.d.), both of which were made of stainless steel. The gap between the needle tip and the center of the ring was 3 mm, and a discharge voltage of −4.5 kV was applied to the needle relative to the ring electrode. The gas mixtures passing through the chamber were then drawn into a nano-DMA with a Faraday cup electrometer (FCE), and the size distributions of the charged particles were measured. In this experiment, particles were measured in a mobility range as low as 10^{-3} cm^2 V^{-1} s^{-1}, which corresponded to particle diameters as large as about 30 nm.

For the measurement of ion mass spectra, the same gas mixtures were introduced into the drift tube of the IMS/MS. The ion source was placed at the end of the drift tube. Ions that enter the drift tube travel along the electric field and can react with surrounding neutral molecules until being sampled into the mass spectrometer through an orifice plate. Thus, the reaction time of ions depends on the length of the drift region, the intensity of the electric field, and the mobility of the ions. For negative ions generated by a radioactive source of ^{241}Am, the measurements were conducted at a fixed ion reaction time (ca. 9 ms). With the corona ion source, we measured ion mass spectra with two different reaction times (ca. 0.6 and 14 ms), and investigated the evolution of negative ions. The highest mass of ions measurable with the mass spectrometer was m/z = 1000. This was not sufficient to analyze the composition of charged particles formed in this study. For example, a cluster ion with a diameter as small as 1 nm is expected to be composed of more than 100 molecules. Therefore, the mass spectrometer was used mainly to investigate the kinetics of ion-molecule reactions involving SO_2. By comparing the mass spectra obtained with the mobility distributions of particles, we deduced the identity of the ion species responsible for charged-particle formation.

3. Results and discussion

3.1. Ionization by α-ray irradiation from ^{241}Am

The mobility of negatively charged particles produced by α-ray irradiation is shown as a function of H_2O concentration in Fig. 2a–c. The concentration of SO_2 was 5 ppm. The particles showed a unimodal distribution at [H_2O] = 20 ppm, the center of which was about 2.0 cm^2 V^{-1} s^{-1}. No signal was observed in the mobility range below 0.6 cm^2 V^{-1} s^{-1}. This indicates that only molecular and cluster ions were present and that no particle formation occurred at the lowest H_2O concentration. As H_2O concentration increased, the distribution turned bimodal. Particles with lower mobility appeared between 0.85 and 0.03 cm^2 V^{-1} s^{-1}, which corresponded to a particle diameter of 1.6–7 nm. It was noteworthy that the appearance of particle signals accompanied a slight decline of the ions with a mobility between 2.0 and 1.0 cm^2 V^{-1} s^{-1}. This change in mobility reflected the nucleation process of large cluster ions becoming charged fine particles. The critical mobility value for nucleation in this case was approximately 0.81 cm^2 V^{-1} s^{-1} (∼1.6 nm).

The corresponding mass spectra of negative ions are shown in Fig. 2d–f. The reaction time of the ions detected was approximately 9 ms. No significant ion signal was observed in the mass range lower than m/z = 50 and more than 300. In dry conditions (Fig. 2d), the observed ions were SO_2^- (m/z = 64), SO_3^- (80), SO_4^- (96), and SO_5^- (112), all of which can be formed through ion-molecule reactions involving SO_2. The primary ions of O_2^- and $O_2^-(H_2O)_n$ generated

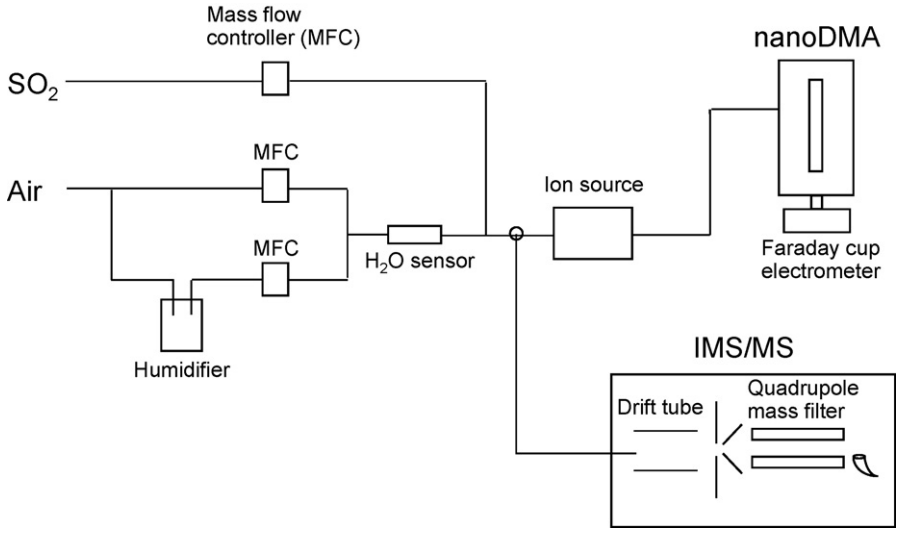

Fig. 1. Schematic diagram of the experimental setup.

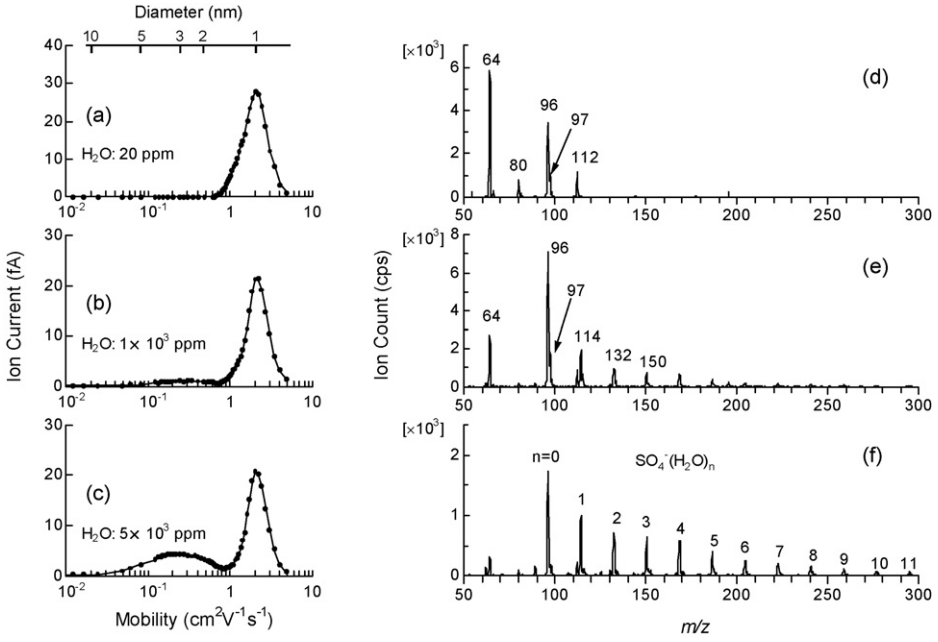

Fig. 2. Mobility distributions of negatively charged particles (left column) and corresponding mass spectra of negative ions (right column) obtained with a radioactive ion source (^{241}Am) at three different H_2O concentrations. $[SO_2] = 5$ ppm.

by the ionization of air reacted with SO_2 to form the ions of SO_2^- and subsequently SO_4^- [22,23]:

$$O_2^- + SO_2 \rightarrow SO_2^- + O_2 \qquad k_1 = 2.0 \times 10^{-9}\,\mathrm{cm^3/s} \tag{1}$$

$$SO_2^- + O_2 + N_2 \rightarrow SO_4^- + N_2 \quad k_2 = 1.0 \times 10^{-12}\,\mathrm{cm^3/s}$$
$$(\text{effective binary rate constant, } 2.5\,\mathrm{h\,Pa,\ 298\,K}) \tag{2}$$

$$O_2^- \cdot H_2O + SO_2 \rightarrow SO_4^- + H_2O \qquad k_3 = 1.8 \times 10^{-9}\,\mathrm{cm^3/s} \tag{3}$$

The ions of SO_3^- can result from the reaction of SO_2 with O_3^- and CO_3^- as follows [22]:

$$O_3^- + SO_2 \rightarrow SO_3^- + O_2 \qquad k_4 = 1.9 \times 10^{-9}\,\mathrm{cm^3/s} \tag{4}$$

$$CO_3^- + SO_2 \rightarrow SO_3^- + CO_2 \qquad k_5 = 4.8 \times 10^{-10}\,\mathrm{cm^3/s} \tag{5}$$

The conversion from SO_3^- to SO_5^- could proceed rapidly by the following three-body process, hence, the lifetime of SO_3^- was extremely short [22]:

$$SO_3^- + O_2 + N_2 \rightarrow SO_5^- + N_2 \qquad k_6 = 2.0 \times 10^{-12}\,\mathrm{cm^3/s}$$
$$(\text{effective binary rate constant, } 2.5\,\mathrm{h\,Pa,\ 298\,K}) \tag{6}$$

The abundance of the ions of SO_2^- and SO_4^- were considerably larger than those of SO_3^- and SO_5^-, showing that O_2^- ions were the dominant primary ions produced by α-ray irradiation in air.

Another ion we can find in the spectrum is HSO_4^- ($m/z = 97$), indicating the formation of sulfuric acid (H_2SO_4). H_2SO_4 is produced mostly by the gas phase oxidizing reaction of SO_2 with OH radicals:

$$SO_2 + OH + M \rightarrow HSO_3 + M \tag{7}$$

$$HSO_3 + O_2 \rightarrow SO_3 + HO_2 \tag{8}$$

$$SO_3 + H_2O + M \rightarrow H_2SO_4 + M \tag{9}$$

The reaction (8) is normally very fast and the lifetime of the intermediate product of HSO_3 is only 0.5 μs in air [24]. The reaction (9) proceeded less rapidly depending on H_2O concentration, which allowed SO_3 to persist much longer than HSO_3.

The ions of SO_3^- and SO_5^- declined with increasing H_2O concentration, as shown in Fig. 2e. By contrast, the hydrated ions of SO_4^- started to appear and became increasingly dominant in the spectra as H_2O concentration increased, as seen in Fig. 2f. This change in ion composition was likely due to the enhancement of $O_2^-(H_2O)_n$ in the primary ion formation by the addition of H_2O. On the other hand, the cluster ion of $HSO_4^-(H_2O)_n$ can be observed only in minor numbers and became negligible as the H_2O increased. This result indicates that ionization by α-ray irradiation provides little OH formation, and, therefore, has a very small oxidizing capability. From the measured mass spectra, it can be concluded that charged particles observed in the mobility distributions were formed via the ion-induced nucleation of SO_4^- cluster ions. It should be noted that cluster ions of $SO_4^-(H_2O)_n$ with a n larger than 11 hardly appeared in the spectrum, as shown in Fig. 2f, whereas the mobility measurement demonstrated the formation of the charged particles larger than 2 nm under the same conditions. One of the reason for the larger cluster ions not being observed in the mass spectrum may be attributed to the short reaction time of ions measured using the mass spectrometer (ca. 9 ms) compared with that of the charged particles measured using the DMA (a few hundreds of milliseconds).

3.2. Ionization by negative dc corona discharge

The mobility of charged particles produced by negative corona discharge differed significantly from those produced by α-ray irradiation. Fig. 3a shows how mobility depends on H_2O concentration at $[SO_2] = 1$ ppm. The mobility distribution when $[H_2O] = 30$ ppm was very similar to that produced by α-ray irradiation (see Fig. 2a) with a single peak centered at about 2.0 $\mathrm{cm^2\,V^{-1}\,s^{-1}}$. Thus, no charged-particle formation was observed under these conditions. In contrast to the results from an α-ray source, however, an increase in H_2O concentration led to considerable nucleation. Both the number and the size of the formed particles significantly increased with the addition of H_2O. The signal corresponding to gaseous ions disappeared and unimodal distributions centering at about 0.99 $\mathrm{cm^2\,V^{-1}\,s^{-1}}$ (1.4 nm in particle diameter) and

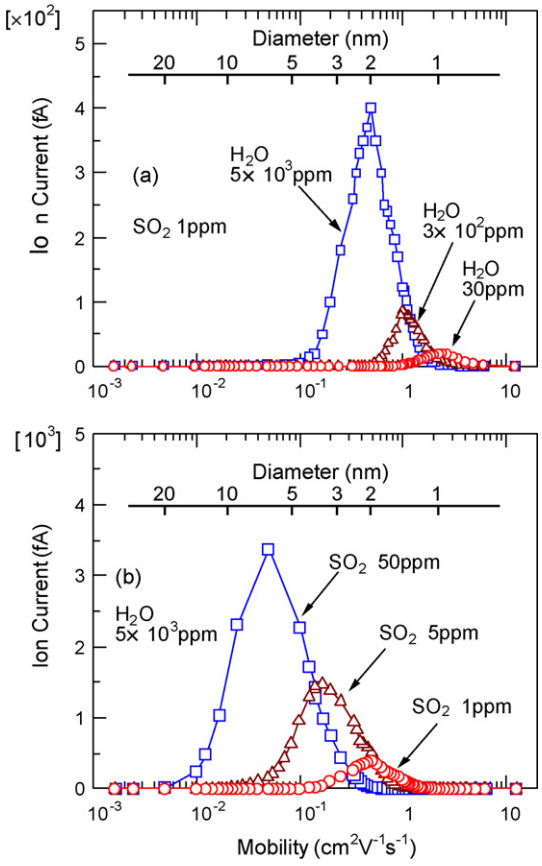

Fig. 3. Mobility distributions of negatively charged particles produced by negative corona discharge. (a) $[SO_2] = 1$ ppm and (b) $[H_2O] = 5 \times 10^3$ ppm.

0.49 $cm^2\,V^{-1}\,s^{-1}$ (2.0 nm) were observed at $[H_2O] = 3 \times 10^2$ and 5×10^3 ppm, respectively.

The change in mobility distribution of particles as a function of SO_2 concentration is shown in Fig. 3b. Both the formation and the growth of charged particles were greatly enhanced by an increase in SO_2 concentration. When $[SO_2] = 5$ ppm and $[H_2O] = 5 \times 10^3$ ppm, the particles were distributed between 1 and 0.02 $cm^2\,V^{-1}\,s^{-1}$. This mobility range is similar to that of the particles formed by α-ray irradiation at the same SO_2 and H_2O concentrations, as shown in Fig. 2c. The number of the particles formed by corona discharge was, however, more than two orders of magnitude greater. The peak mobility fell as low as 0.05 $cm^2\,V^{-1}\,s^{-1}$ when $[SO_2] = 50$ ppm.

The mass spectra of negative ions generated by negative corona discharge are shown in Fig. 4. We measured the spectra using two reaction times at $[SO_2] = 5$ ppm. The majority of the ion signals was observed in the mass range below $m/z = 300$. Fig. 4a–c shows the dependence on H_2O concentration of the mass spectra with a short ion reaction time (0.6 ms). The spectra were simple, especially at low H_2O concentrations. While the presence of SO_x^- ions ($x = 2$–5) was the same as the spectra obtained when using a radioactive ion source, the relative abundance of these ions was significantly different. The ions of SO_5^- appeared to have the highest intensity for all the spectra, whereas the ions of SO_2^- and SO_4^-, which predominated in the mass spectra with an α-ray ion source, were present in much smaller amounts. In the negative ion mass spectra obtained in the absence of SO_2, the relative abundance of O_2^- was much smaller than that of O_3^- under conditions of low H_2O concentration, being less than 8% of total ions. Consequently, the reaction of SO_2 with O_2^- was less important in negative corona discharge compared to ionization by α-rays. In addition to the SO_x^- ions, HSO_4^- ($m/z = 97$) was also found, albeit in small numbers, in the spectra with short reaction times. Most of the detected ions were clustered with water molecules at $[H_2O] = 3 \times 10^3$ ppm.

Two other ion peaks, which may have resulted from the reactions involving SO_2, were observed at $m/z = 81$ and 113, although in relatively small numbers. As judged from their masses, these ions could be HSO_3^- and HSO_5^-. Reportedly, OH^- ions react rapidly with SO_2 to form HSO_3^- ions [25]:

$$OH^-(H_2O)_n + SO_2 \rightarrow HSO_3^-(H_2O)_{n-1} + H_2O$$

$$k_{10} = 2 \times 10^{-9}\ cm^3/s \quad (10)$$

In our previous study with a negative corona source, the formation of $OH^-(H_2O)_n$ ions was confirmed in purified air [21]. Several reactions are capable of forming OH^- ions from negative corona discharges in air. Recently, Skalny et al. [17] proposed the following two-step process:

$$O^- + H_2O + O_2 \rightarrow O^-{\cdot}H_2O + O_2 \qquad k_{11} = 1.3 \times 10^{-28}\ cm^6/s \quad (11)$$

$$O^-{\cdot}H_2O + H_2O \rightarrow OH^-{\cdot}H_2O + OH \qquad k_{12} > 1 \times 10^{-11}\ cm^3/s \quad (12)$$

Another process that may contribute to the formation of HSO_3^- is the following:

$$SO_2^- + OH + M \rightarrow HSO_3^- + M \quad (13)$$

Unfortunately, data were not available to evaluate the possibility of this reaction in the present experiment. Little information exists on the formation mechanism of HSO_5^-. We can only assume a process similar to reaction (13):

$$SO_4^- + OH + M \rightarrow HSO_5^- + M \quad (14)$$

The ion of NO_3^- ($m/z = 62$) was the only ion that did not originate from SO_2. The formation of this ion was negligible with α-ray irradiation. Under conditions of low H_2O concentration, NO_3^- can be formed by the following reactions [23]:

$$NO_2^- + O_3 \rightarrow NO_3^- + O_2 \qquad k_{15} = 1.2 \times 10^{-10}\ cm^3/s \quad (15)$$

$$O_3^- + NO_2 \rightarrow NO_3^- + O_2 \qquad k_{16} = 2.8 \times 10^{-10}\ cm^3/s \quad (16)$$

The reactions of O^- with NO_2 and O_3, both of which are major byproducts in air discharges, normally yield NO_2^- and O_3^-, respectively. In our previous study, an enhancement of HNO_3 formation was observed with increasing H_2O concentration probably through reaction [21]:

$$NO_2 + OH + M \rightarrow HNO_3 + M \qquad k_{17} = 3.3 \times 10^{-30}\ cm^6/s \quad (17)$$

HNO_3 has a large electron affinity for the formation of NO_3^- ions by charge transfer reactions with other negative ions such as [23]:

$$NO_2^- + HNO_3 \rightarrow NO_3^- + HNO_2 \qquad k_{18} = 1.6 \times 10^{-9}\ cm^3/s \quad (18)$$

Almost all the possible reactions forming OH in discharge plasma require H_2O. In addition to reactions (11) and (12), dissociation of H_2O by electron impact can directly form OH radicals:

$$e + H_2O \rightarrow OH + H + e \quad (19)$$

The rate coefficient of this reaction depends on the intensity of the reduced electric field in the discharge area. The electron impact on O_2 yields excited oxygen atoms, $O(^1D)$:

$$e + O_2 \rightarrow O(^1D) + O(^3P) + e \quad (20)$$

Dissociation of H_2O by $O(^1D)$ can contribute to OH formation [26]:

$$O(^1D) + H_2O \rightarrow 2OH \qquad k_{21} = 2.2 \times 10^{-10}\ cm^3/s \quad (21)$$

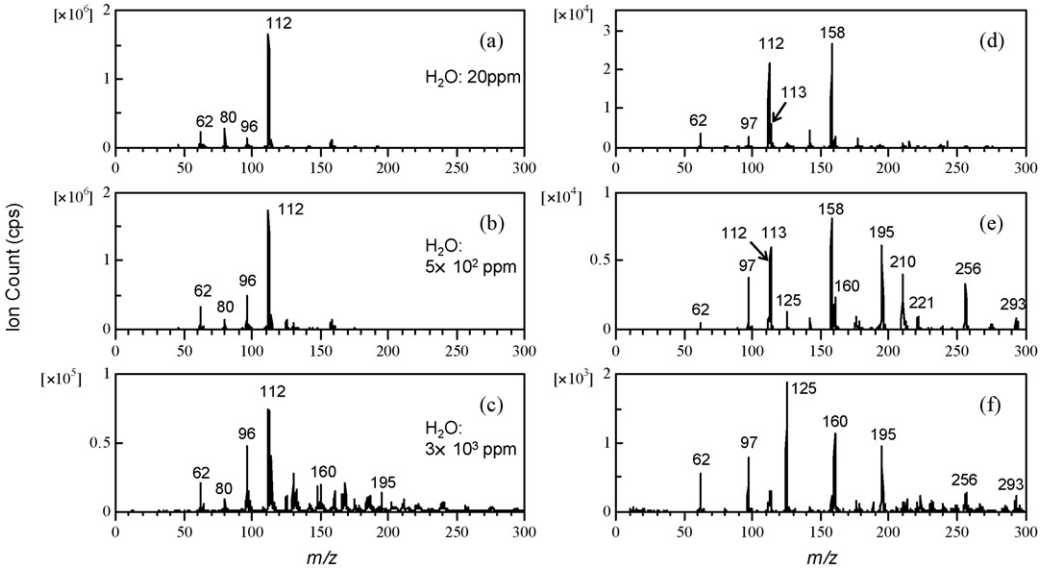

Fig. 4. Mass spectra of negative ions produced by negative corona discharge with $[SO_2] = 5$ ppm at three different H_2O concentrations: (a and d) 20 ppm, (b and e) 5×10^2 ppm, (c and f) 3×10^3 ppm. The reaction times of ions are approximately 0.6 ms for spectra (a–c), and 14 ms for spectra (d–f), respectively. m/z = 62: NO_3^-, 80: SO_3^-, 96: SO_4^-, 97: HSO_4^-, 112: SO_5^-, 113: HSO_5^-, 125: $NO_3^-HNO_3$, 158: $SO_5^-NO_2$, 160: $HSO_4^-HNO_3$, 195: $HSO_4^-H_2SO_4$, 210: $SO_5^-H_2SO_4$, 221: $SO_5^-NO_2HNO_3$, 256: $SO_5^-NO_2H_2SO_4$, 293: $HSO_4^-(H_2SO_4)_2$.

Some fractions of OH^- ions formed by reactions (11) and (12) transfer the charge by the reactions with NO_2 and O_3 to yield neutral OH radicals. As a consequence, an increase in H_2O concentration accelerates the transformation from NO_2 to HNO_3, which plays a major role in the formation of NO_3^- ions under conditions of higher H_2O concentration. HNO_3 not only contributes to the formation of NO_3^- core ions, but it also tends to associate with other stable ions. In our spectra, ions of $NO_3^-HNO_3$ (m/z = 125), $HSO_4^-HNO_3$ (160) and $SO_5^-HNO_3$ (175) were observed. These ions were hydrated at higher H_2O concentrations.

The detected ions were classified into eight groups with different core ions of NO_3^-, SO_2^-, SO_3^-, HSO_3^-, SO_4^-, HSO_4^-, SO_5^-, and HSO_5^-. Fig. 5a shows the changes in relative abundance of each ion group as a function of H_2O concentration.

The abundance of the SO_4^- ions significantly increased with H_2O concentration. This is a tendency that is similar to that observed in the spectra obtained using an α-ray ion source. In the spectra of negative corona discharge measured without SO_2, however, O_2^- ions did not show a remarkable increase and remained a minor ion species. Therefore, paths other than reactions (2) and (3) may yield SO_4^- ions. The following reaction possibly contributes to the formation of SO_4^- ions [27]:

$$NO_3^- + SO_3 \rightarrow SO_4^- + NO_2 \qquad k_{22} = 9.6 \times 10^{-10}\ \mathrm{cm^3/s} \qquad (22)$$

As mentioned above, in conditions with higher H_2O concentrations, the formation of NO_3^- ions is favored. In fact, in the present study, they were observed to be the most dominant ion species in the mass spectrum measured without SO_2 at $[H_2O] = 3 \times 10^3$ ppm. In addition, the formation of SO_3 is also expected to be enhanced by the addition of H_2O because it starts with the reaction of SO_2 and OH (see reactions (7) and (8)). Therefore, higher H_2O concentrations may favor the reaction (22).

Another group that increased with H_2O was HSO_4^- ions. This also can be attributed to the enhancement of OH formation and its subsequent formation of H_2SO_4. Core change reactions of negative ions such as NO_3^- with H_2SO_4 to form HSO_4^- are known to proceed rapidly because of the large electron affinity of H_2SO_4. In addition, H_2SO_4 molecules tend to cluster with negative ions. In the measured spectra, clustered ions of $HSO_4^-H_2SO_4(H_2O)_n$ and $SO_5^-H_2SO_4(H_2O)_n$ were observed. It should be noted that the ratio of the relative number of HSO_4^- ions to that of SO_4^- ions in the spectra was significantly higher compared with that in the spectra measured using an α-ray source. This clearly indicates that negative corona discharge has a much higher oxidizing capability than does ^{241}Am.

The ion group of SO_5^-, to the contrary, was greatly reduced when H_2O was increased. One of the reasons may be attributed to a remarkable drop in the relative abundance of O_3^- among the primary ions with the addition of H_2O, which was observed in the mass

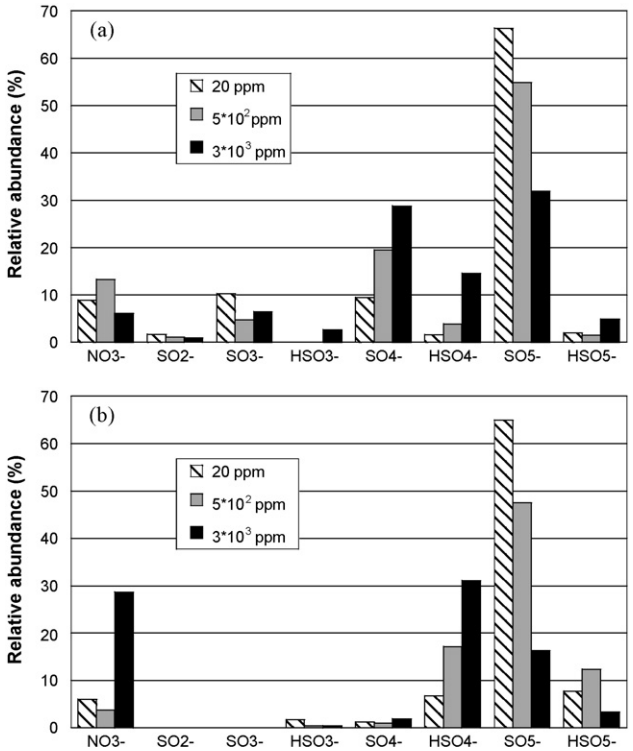

Fig. 5. Relative abundance of ion groups as a function of H_2O concentration at two different ion reaction times of 0.6 ms (a) and 14 ms (b).

spectra obtained without SO_2. The reduction of O_3^- can apparently make reaction (4), and subsequently reaction (6), less active.

SO_3^- ions, however, did not show a great reduction with an increase in H_2O concentration. Other mechanisms may explain the decline in SO_5^- ions. One possibility is the conversion of SO_5^- to ions such as HSO_4^- and HSO_5^-, both of which increased with H_2O concentration. Eisele et al. recently proposed the possibility of an unknown reaction of SO_5^- and H_2SO_4 to form $HSO_4^-H_2SO_4$ under SO_2-rich conditions [3]. If this kind of reaction works effectively, the transformation from SO_5^- ions to HSO_4^- ions could proceed at high H_2O concentrations.

The mass spectra with a long reaction time (14 ms) are shown in Fig. 4d–f. The ion of $m/z = 158$ appears prominently, particularly in the mass spectra obtained with the lowest H_2O concentration. The identity of this ion is not clear, but there are several candidates. Salcedo et al. found the $m/z = 158$ ion in the mass spectra obtained in their experiment studying the reaction of CO_3^- and H_2SO_4, and they ascribed it to $H_2SO_4CO_3^-$ [28]. However, the CO_3^- monomer was not present in the mass spectrum shown in Fig. 4d, in which the $m/z = 158$ ion was the most abundant. Moreover, HSO_4^- was observed with a very low abundance in the same mass spectrum, indicating that the production of H_2SO_4 was small. Hence, the $m/z = 158$ ion observed in our spectra is unlikely to be $H_2SO_4CO_3^-$. The $m/z = 158$ ion has been detected in the mass spectra of natural negative ions in the atmosphere. Using a tandem mass spectrometry technique, Eisele and Tanner identified it as $SO_4NO_3^-$ [2]. However, NO_3^- was not abundant in the spectrum shown in Fig. 4d, which does not support the contention that NO_3^- core ions are responsible for the $m/z = 158$ ion in our experiments. On the other hand, the abundance of this ion was observed to decrease coincidentally with that of SO_5^- as H_2O concentration increased, which strongly suggests that this ion belongs to the group of SO_5^- ions. Since no SO_5^- ions having a mass of 158 have been reported, the identity of this ion is yet to be revealed. Judging from its mass, however, $SO_5^-NO_2$ is a possible candidate. Then, we tentatively labeled this ion as $SO_5^-NO_2$, although further investigation is required to confirm this identification. We use this assignment in the following discussions.

In the mass spectrum shown in Fig. 4e, cluster ions having neutral HNO_3 or H_2SO_4 molecules are dominant. Those ions include $NO_3^-HNO_3$ ($m/z = 125$), $HSO_4^-HNO_3$ (160), $HSO_4^-H_2SO_4$ (195), $SO_5^-H_2SO_4$ (210), $SO_5^-NO_2HNO_3$ (221), $SO_5^-NO_2H_2SO_4$ (256), and $HSO_4^-(H_2SO_4)_2$ (293). Since these cluster ions were not observed in the spectra with a short reaction time, the formation of the cluster ions with HNO_3 or H_2SO_4 molecules took at least a few milliseconds under the present experimental conditions of $[H_2O] = 5 \times 10^2$ ppm. A further increase in H_2O concentration led to the dominance of cluster ions with HNO_3 such as $NO_3^-HNO_3$ and $HSO_4^-HNO_3$, as shown in Fig. 4f.

The results of ion evolution from 0.6 to 14 ms are illustrated in Fig. 5b. The ions of SO_2^- and SO_3^- disappeared, indicating that these ions were completely transformed into SO_4^- and SO_5^-, respectively, within the reaction time of 14 ms. In addition, the ion group of SO_4^-, which comprised one of the major ion species in the mass spectrum with a short reaction time and high humidity, was reduced significantly. This means that SO_4^- ions were transformed further into other ions as reaction time increased, and their lifetimes are relatively short. The ions of SO_5^- also were reduced with reaction time: the degree of reduction became larger as H_2O concentration increased. On the other hand, the relative abundance of HSO_4^- ions increased about 2–3 times depending on H_2O concentration. At $[H_2O] = 3 \times 10^3$ ppm, HSO_4^- ions surpassed the ions of other groups. These results seem to show that, particularly under conditions of high H_2O concentration, the conversions from SO_4^- and SO_5^- ions to HSO_4^- will proceed. The reactions of SO_4^- and SO_5^- with H_2SO_4 are probably responsible for the conversions, but little is known about these reactions. The ions of HSO_5^- also increased with reaction time except in the case of the highest H_2O concentration.

Interestingly, the ions of NO_3^- increased approximately five times with reaction time at $[H_2O] = 3 \times 10^3$ ppm, whereas they declined at lower H_2O concentrations. As Fig. 4f shows, $NO_3^-HNO_3$ was the most abundant ion. In addition, $HSO_4^-HNO_3$ was the most abundant among the ions having an HSO_4^- core, which was the most dominant ion group. It is evident that the formation of HNO_3 was significantly enhanced under these conditions. Since the relative abundance of NO_3^- groups was only about 6% with a short reaction time, it seems that some of the SO_x^- ions were converted into NO_3^- ions by the reaction with HNO_3. It is reported that HNO_3 rapidly reacts with SO_3^- and SO_4^-, but these reactions yield mostly clustered ions of $SO_3^-HNO_3$ and $SO_4^-HNO_3$ [25,29]. Further studies are required to explain the remarkable enhancement of NO_3^- ions with the reaction times observed in the present experiment.

4. Conclusions

In this paper, we presented the results of the measurement of charged particles formed by the ionization of air containing SO_2. For both ion sources used in this experiment, ^{241}Am and negative dc corona discharge, the formations of charged particles increased as H_2O concentration increased. However, the efficiency of particle formation was significantly different, and the number of particles formed by negative corona discharge was more than two orders of magnitude larger than those formed by ^{241}Am. Therefore, care should be taken when using a monopolar charger employing a corona source for the measurement of aerosols in the air containing impurities that can be transformed into condensable compounds by the effects of ionization.

The composition of negative ions generated using ^{241}Am in the SO_2/H_2O/air mixture was rather simple. $SO_4^-(H_2O)_n$ ions became increasingly dominant with increasing H_2O concentration, and the charged particles were likely formed through ion-induced nucleation around these ions. In charged particle formation by α-ray irradiation, therefore, the main role of H_2O is in the formation of hydrated ion clusters.

By contrast, the negative ion mass spectra measured using a corona ion source were complex and contained a variety of cluster ions. Major ion groups included NO_3^-, SO_x^- ($x = 2$–5), and HSO_x^- ($x = 3$–5), and the relative abundance of the ion groups varied depending on H_2O concentration and ion reaction time. The dominance of cluster ions of HSO_4^- and NO_3^- with ligands of H_2SO_4 and HNO_3 at higher H_2O concentrations suggests that H_2O plays an important role as a source of OH radicals in the case of negative corona discharge.

Acknowledgements

The author wishes to thank T. Kawabuchi and Y. Ohara for their assistance in the experiments. This work was sponsored by a Grant-in-Aid for Scientific Research from The Ministry of Education, Culture, Sports, Science and Technology of Japan (14048227, 16030214, 20510018).

References

[1] M.B. Enghoff, H. Svensmark, Atmos. Chem. Phys. 8 (2008) 4911.
[2] F.L. Eisele, D.J. Tanner, J. Geophys. Res. 95 (1990) 20539.
[3] F.L. Eisele, E.R. Lovejoy, E. Kosciuch, K.F. Moore, R.L. Mauldin III, J.N. Smith, P.H. McMurry, K. Iida, J. Geophys. Res. 111 (2006) D04305, doi:10.1029/2005JD006568.
[4] K. Iida, M. Stolzenburg, P. McMurry, M.J. Dunn, J.N. Smith, F. Eisele, P. Keady, J. Geophys. Res. 111 (2006) D23201, doi:10.1029/2006JD007167.
[5] L. Laakso, S. Gagné, T. Petäjä, A. Hirsikko, P.P. Aalto, M. Kulmala, V.-M. Kerminen, Atmos. Phys. Chem. 7 (2007) 1333.

[6] J.Y. Park, I. Tomicic, G.F. Round, J.S. Chang, J. Phys. D: Appl. Phys. 32 (1999) 1006.
[7] Z. Zhang, M. Bai, M. Bai, X. Bai, Q. Pan, J. Air Waste Manage. Assoc. 56 (2006) 810.
[8] A.B. Saveliev, G.J. Pietsch, A.R. Murtazin, A. Fried, Plasma Sources Sci. Technol. 16 (2007) 454.
[9] K.G. Vohra, M.C. Subba Ramu, T.S. Muraleedharan, Atmos. Environ. 8 (1984) 1653.
[10] G.L. Diamond, J.V. Iribarne, D.J. Corr, J. Aerosol Sci. 16 (1985) 43.
[11] J.M. Mäkelä, Radiat. Phys. Chem. 40 (1992) 301.
[12] S.C. Yoon, W.H. Marlow, P.K. Hopke, Health Phys. 60 (1992) 51.
[13] T.O. Kim, M. Adachi, K. Okuyama, J.H. Seinfeld, Aerosol Sci. Technol. 26 (1997) 527.
[14] H. Svensmark, J.O.P. Pedersen, N.D. Marsh, M.B. Seinfeld, U.I. Uggerhøj, Proc. Roy. Soc. A 463 (2007), doi:10.1098/rspa.2006.1773.
[15] S.K. Ross, A.J. Bell, Int. J. Mass Spectrom. 218 (2002) L1.
[16] J.D. Skanly, T. Mikoviny, S. Matejcik, N.J. Mason, Int. J. Mass Spectrom. 233 (2004) 317.
[17] J.D. Skalny, J. Orszagh, S. Matejcik, N.J. Mason, J.A. Rees, Y. Aranda-Gonzalvo, T.D. Whitmore, Int. J. Mass Spectrom. 272 (2008) 12.
[18] K. Nagato, C.S. Kim, M. Adachi, K. Okuyama, J. Aerosol Sci. 36 (2005) 1036.
[19] M. Adachi, K. Kousaka, K. Okuyama, J. Aerosol Sci. 16 (1985) 109.
[20] A. Hernandez-Sierra, F.J. Alguacil, M. Alonso, J. Aerosol Sci. 34 (2003) 733.
[21] K. Nagato, Y. Matsui, T. Miyata, T. Yamauchi, Int. J. Mass Spectrom. 248 (2006) 142.
[22] O. Möhler, T. Reiner, F. Arnold, J. Chem. Phys. 97 (1992) 8233.
[23] Y. Ikezoe, S. Matsuoka, M. Takebe, A.A. Viggiano, Gas Phase Ion-Molecule Reaction Rate Constants Through 1986, Maruzen, Tokyo, 1987.
[24] B.J. Finlayson-Pitts, J.N. Pitts Jr., Chemistry of the Upper and Lower Atmosphere, Academic Press, San Diego, CA, USA, 2000.
[25] F.C. Fehsenfeld, E.E. Ferguson, J. Chem. Phys. 61 (1974) 3181.
[26] R. Atkinson, D.L. Baulch, R.A. Cox, J.N. Crowley, R.F. Hampson, R.G. Hynes, M.E. Jenkin, M.J. Rossi, J. Troe, Atmos. Chem. Phys. 4 (2004) 1461.
[27] S.T. Arnold, R.A. Morris, A.A. Viggiano, J. Geophys. Res. 100 (1995) 14141.
[28] D. Salcedo, P.W. Villalta, V. Varutbangkul, J.C. Wormhoudt, R.C. Miake-Lye, D.R. Worsnop, J.O. Ballenthin, W.F. Thorn, A.A. Viggiano, T.M. Miller, R.C. Flagan, J.H. Seinfeld, Int. J. Mass Spectrom. 231 (2004) 17.
[29] F.C. Fehsenfeld, C.J. Howard, A.L. Schmeltekopf, J. Chem. Phys. 63 (1975) 2835.